SUPPLEMENTARY MATERIAL

Non-Nuclear Attractors in Small Charged Lithium Clusters, Li_m^q (m = 2-5, q = ±1), with QTAIM and the Ehrenfest Force Partitioning

Alireza Azizi, Roya Momen, Tianlv Xu, Steven R. Kirk* and Samantha Jenkins*

[1]*Key Laboratory of Chemical Biology and Traditional Chinese Medicine Research and Key Laboratory of Resource Fine-Processing and Advanced Materials of Hunan Province of MOE, College of Chemistry and Chemical Engineering, Hunan Normal University, Changsha Hunan 410081, China.*

e-mail: steven.kirk@cantab.net

e-mail: samanthajsuman@gmail.com

1. Supplementary Materials S1. Computational protocol and numerical evaluation of the Ehrenfest force **F**(**r**) partitioning.

2. Supplementary Materials S2. Tabulated QTAIM partitioning scheme measures for the molecular graphs of the Li_m^q (m = 2-5, q = ±1) clusters.

3. Supplementary Materials S3. Tabulated Ehrenfest Force **F**(**r**) partitioning scheme measures for the molecular graphs of the Li_m^q (m = 2-5, q = ±1) clusters.

4. Supplementary Materials S4. Variation of the total charge density difference ($\rho(\mathbf{r}_a)$-$\rho(\mathbf{r}_b)$) with *NNA-BCP* separation for the Li_m^q (m = 2-5, q = ±1)

5. Supplementary Materials S5. Variation of the metallicity $\xi(\mathbf{r}_b)$ with the *NNA-BCP* separation of the Li_m^q (m = 2-5, q = ±1) clusters.

6. Supplementary Materials S6. QTAIM measures of stretched molecular graphs of the Li_2^- cluster.

7. Supplementary Materials S7. QTAIM measures of compressed molecular graphs of the Li_2^+ cluster.

8. Supplementary Materials S8. Ehrenfest partitioning measures for the stretched molecular graphs of the Li_2^+ cluster.

1. Supplementary Materials S1. Computational protocol and numerical evaluation of the Ehrenfest force **F**(**r**) partitioning

The inherent difficulties of the computation of the Ehrenfest force **F**(**r**) were examined during a previous investigation by some of the current authors,[1] attributing the spurious artifacts to the diffuse GTOs used in basis sets. Research has been undertaken in accurately computing quantum stress tensor properties using Gaussian basis sets. In the work by Tachibana *et al*.,[2] they studied the effect of the basis sets expansion on the electronic stress tensor calculations, compared with the exact wave function for the ion H+ 2, showing that the calculations for *cc*-pV5Z and *cc*-pV6Z basis sets are in close agreement with the *spindle* form of the exact wave function. In addition, other authors[3] showed the effect of the basis sets on the stress tensor, calculating the profiles of the magnitude of the attractive **F**(**r**) for the H and H_2 ground states. In this case, the expanded basis set aug-*cc*-pV5Z provided the best agreement with the exact computation of **F**(**r**). It was suggested in 2007 by Hernández-Trujillo and co-workers that spurious artifacts are pushed into the bonding regions upon close-approach of the nuclei[4] in the **F**(**r**) calculations if GTOs with s and p functions with exponents of order of 10^5 and 10^3 were used. This can be contrasted with conventional basis sets such as pV6Z which have exponent values of order 10^3 and 10^1 respectively. Following that suggestion we decided to use the extended relativistic Atomic Natural Orbital (ANO-RCC) GTO basis sets developed by Ross and collaborators.[5–7] These basis sets were constructed by averaging over several atomic states, positive and negative ions and atoms in an external electric field, with the key feature that they are highly focused at the nuclei.

(i) Computational protocol

Previously, as a starting point, some of the current authors, decided that the standard *cc*-pV5Z and *cc*-pV6Z basis sets cannot be modified by removing the same number of exponents in each GTO.[1] This was because in these basis sets the same kind of Gaussian functions have different numbers of exponents, thus an uneven modification of the standard basis sets causes a loss of the functional nature of the basis set. The ANO-RCC basis sets, however, have the same number of exponents in each GTO, allowing us to remove the same number of exponents from each function in the GTO. For each atom the basis sets were rewritten into the form of the standard basis sets (*cc*-pVXZ(X = D,T,Q)), then only exponents in a specific range for each function were kept and the others removed. This yielded a new kind of modified ANO RCC basis set where the highly focused functions prevail over diffuse functions. Thus each atom has an *engineered* ANO-RCC basis set: values for the preserved exponents in each basis set can be found in our previous contribution.[1] These values were determined by calculation of the **F**(**r**) trajectories for each modified basis set with different ranges of exponents until a well-behaved set of **F**(**r**) (free of spurious features) was obtained.

(ii) Numerical evaluation of the Ehrenfest force F(r) Partitioning Scheme

A convenient start point is the simple system, H_2, which is a highly symmetrical molecule, with an Ehrenfest *BCP* halfway between the two hydrogen nuclei. Fig. 1 shows the Ehrenfest force trajectory calculation for the H_2 molecule. In Fig. 1(a) and (b) the aug-*cc*-pVQZ basis set and the non-modified ANO-RCC basis sets were respectively used. These basis sets contain diffuse functions and despite the fact that in the ANO-RCC the functions are more localized at the nuclei than in the aug-*cc*-pVQZ, the appearance of spurious features evidenced a strong dependence of the computation of the **F**(**r**) on the presence of diffuse functions in the basis sets. The *cc*-pVQZ basis set contains 10 GTOs (4s,3p,2d,1f) while ANO-RCC contains 16 GTOs (8s,4p,3d,1f) and although the shape of the **F**(**r**) trajectories is mostly the same, the location of the spurious features changes by 1 a.u., further away from the nuclei. The original aug-*cc*-pVQZ was not modified and therefore not shown (for details refer to subsection (i)), Fig. 1(c) shows the modified ANO-RCC basis (for the values in the preserved exponents[1]). The plot does not contain any spurious surfaces and a monotonic behaviour of the **F**(**r**) is apparent. Considering that higher order derivatives used in the computation of the **F**(**r**) may act to magnify errors in the **F**(**r**) calculation, to ensure a correct calculation, the researcher should be particularly careful with the critical point properties calculated from the optimized geometries.

References

1 J. R. Maza, S. Jenkins, S. R. Kirk, J. S. M. Anderson and P. W. Ayers, The Ehrenfest force topology: a physically intuitive approach for analyzing chemical interactions, Phys. Chem. Chem. Phys., 2013, 15, 17823–17836.

2 K. Ichikawa, A. Wagatsuma, M. Kusumoto and A. Tachibana, Electronic stress tensor of the hydrogen molecular ion: Comparison between the exact wave function and approximate wave functions using Gaussian basis sets, Journal of Molecular Structure: THEOCHEM, 2010, 951, 49–59.

3 A. M. Pendás and J. Hernández-Trujillo, The Ehrenfest force field: Topology and consequences for the definition of an atom in a molecule, The Journal of Chemical Physics, 2012, 137, 134101.

4 J. Hernández-Trujillo, F. Cortés-Guzmán, D.-C. Fang and R. F. W. Bader, Forces in molecules, Faraday Discuss., 2007, 135, 79–95; discussion 125-149, 503–506.

5 P.-O. Widmark, P.-Å. Malmqvist and B. O. Roos, Density matrix averaged atomic natural orbital (ANO) basis sets for correlated molecular wave functions, Theoret. Chim. Acta, 1990, 77, 291–306.

6 B. O. Roos, V. Veryazov and P.-O. Widmark, Relativistic atomic natural orbital type basis sets for the alkaline and alkaline-earth atoms applied to the ground-state potentials for the corresponding dimers, Theor Chem Acc, 2004, 111, 345–351.

7 B. O. Roos, R. Lindh, P.-Å. Malmqvist, V. Veryazov and P.-O. Widmark, New Relativistic ANO Basis Sets for Transition Metal Atoms, J. Phys. Chem. A, 2005, 109, 6575–6579.

2. Supplementary Materials S2.

Table S2. The QTAIM partitioning scheme measures for the molecular graphs of the Li_m^q (m = 2-5, q = ±1) clusters. The total electronic charge density $\rho(\mathbf{r}_a)$ and the Laplacian $\nabla^2\rho(\mathbf{r}_a)$ of the non-nuclear attractor (*NNA*), the total electronic charge density $\rho(\mathbf{r}_b)$, the Laplacian $\nabla^2\rho(\mathbf{r}_b)$ of the bond critical point (*BCP*), total local energy density $H(\mathbf{r}_b)$, metallicity $\xi(\mathbf{r}_b)$, ellipticity ε, atomic units are used.

Li_m^q	*BCP*	Li/*NNA*--*NNA*	*NNA*--*BCP*	$\rho(\mathbf{r}_a)$	$\nabla^2\rho(\mathbf{r}_a)$	$\rho(\mathbf{r}_b)$	$\nabla^2\rho(\mathbf{r}_b)$	$H(\mathbf{r}_b)$	$\xi(\mathbf{r}_b)$	ε
Li_2^-	Li1-*NNA*3	2.5118	0.5994	0.0112	-0.0084	0.0108	0.0027	-0.0020	4.0185	0.7007
	Li2-*NNA*3	2.5118	0.5994	0.0112	-0.0084	0.0108	0.0027	-0.0020	4.0185	0.7007
Li_2^+	Li1-*NNA*3	2.9009	1.0041	0.0126	-0.0129	0.0118	-0.0014	-0.0027	-8.6544	0.0000
	Li2-*NNA*3	2.9009	1.0041	0.0126	-0.0129	0.0118	-0.0014	-0.0027	-8.6544	0.0000
Li_3^-	Li1-*NNA*4	2.5475	0.5891	0.0102	-0.0078	0.0100	0.0003	-0.0017	34.5195	0.0000
	Li2-*NNA*4	3.1396	1.1750	0.0102	-0.0078	0.0094	0.0008	-0.0016	11.3060	0.0000
	Li2-*NNA*5	3.1394	1.1747	0.0102	-0.0078	0.0094	0.0008	-0.0016	11.3033	0.0000
	Li3-*NNA*5	2.5475	0.5892	0.0102	-0.0078	0.0100	0.0003	-0.0017	34.3780	0.0000
Li_3^+	Li1-*NNA*4	3.2136	1.4076	0.0163	-0.0108	0.0145	0.0058	-0.0022	2.5241	0.4534
	Li2-*NNA*4	3.2151	1.4090	0.0163	-0.0108	0.0145	0.0058	-0.0022	2.5231	0.4531
	Li3-*NNA*4	3.2133	1.4072	0.0163	-0.0108	0.0145	0.0058	-0.0022	2.5243	0.4535
Li_4^-	Li1-*NNA*5	3.7071	1.8340	0.0126	-0.0046	0.0107	0.0089	-0.0012	1.2021	0.0004
	Li2-*NNA*5	3.3094	1.4429	0.0126	-0.0046	0.0112	0.0092	-0.0012	1.2144	0.0293
	Li3-*NNA*5	3.3085	1.4420	0.0126	-0.0046	0.0112	0.0092	-0.0012	1.2147	0.0286
	Li4-*NNA*5	3.3095	1.4430	0.0126	-0.0046	0.0112	0.0092	-0.0012	1.2144	0.0293
Li_4^+	Li1-*NNA*5	2.8369	0.9524	0.0135	-0.0091	0.0129	0.0005	-0.0024	24.4951	0.4407
	Li2-*NNA*5	3.5228	1.9004	0.0135	-0.0091	0.0120	0.0058	-0.0017	2.0904	7.2027
	Li2-*NNA*6	3.5234	1.8954	0.0135	-0.0091	0.0120	0.0058	-0.0017	2.0810	6.9050
	Li3-*NNA*5	3.5256	1.9052	0.0135	-0.0091	0.0120	0.0058	-0.0017	2.0916	7.3003
	Li3-*NNA*6	3.5214	1.8919	0.0135	-0.0091	0.0120	0.0058	-0.0017	2.0805	6.8358
	Li4-*NNA*6	2.8370	0.9529	0.0135	-0.0091	0.0130	0.0005	-0.0024	23.6815	0.4409
	*NNA*5-*NNA*6	4.8525	2.4223	0.0135	-0.0091	0.0124	-0.0067	-0.0026	-1.8334	0.5238
			2.4302	0.0135	-0.0091					
Li_5^-(1)	Li1-*NNA*6	3.0358	1.0864	0.0108	-0.0049	0.0102	0.0057	-0.0014	1.7901	53.7352
	Li1-*NNA*7	3.0355	1.0859	0.0108	-0.0049	0.0102	0.0057	-0.0014	1.7907	53.7141
	Li1-*NNA*8	3.0404	1.0916	0.0109	-0.0049	0.0102	0.0057	-0.0014	1.7833	45.4372
	Li1-*NNA*9	3.0326	1.0833	0.0108	-0.0049	0.0102	0.0057	-0.0014	1.7945	57.0982
	Li2-*NNA*8	3.2859	1.6854	0.0108	-0.0049	0.0104	0.0042	-0.0015	2.4640	30.1507
	Li3-*NNA*6	3.2900	1.7529	0.0108	-0.0049	0.0104	0.0042	-0.0015	2.4891	76.7618
	Li4-*NNA*7	3.2861	1.7558	0.0108	-0.0049	0.0104	0.0042	-0.0015	2.4893	78.6665
	Li5-*NNA*8	3.2838	1.6673	0.0108	-0.0049	0.0104	0.0042	-0.0015	2.4609	24.6079
	*NNA*6-*NNA*7	3.2519	1.6937	0.0108	-0.0049	0.0106	-0.0046	-0.0020	-2.2811	0.1865
			1.6911	0.0108	-0.0049					
	*NNA*6-*NNA*8	3.2470	1.6756	0.0108	-0.0049	0.0106	-0.0046	-0.0020	-2.2820	0.1876
			1.7020	0.0109	-0.0049					
	*NNA*7-*NNA*9	3.2407	1.6878	0.0108	-0.0049	0.0106	-0.0047	-0.0020	-2.2798	0.1878
			1.6847	0.0108	-0.0049					

	*NNA*8-*NNA*9	3.2498	1.7067	0.0108	-0.0049	0.0106	-0.0046	-0.0020	-2.2808	0.1858
			1.6746	0.0108	-0.0049					
Li_5^-(2)	Li1-*NNA*6	2.8111	0.9209	0.0120	-0.0083	0.0113	0.0040	-0.0017	2.7951	0.9123
	Li1-*NNA*7	3.9372	2.0942	0.0111	-0.0069	0.0096	0.0044	-0.0012	2.1724	6.2567
	Li2-*NNA*6	2.8114	0.9212	0.0120	-0.0083	0.0113	0.0040	-0.0017	2.7942	0.9118
	Li2-*NNA*8	3.9357	2.0920	0.0111	-0.0069	0.0096	0.0044	-0.0012	2.1723	6.1977
	Li3-*NNA*7	2.6195	0.6950	0.0111	-0.0069	0.0108	0.0021	-0.0016	5.1402	0.9162
	Li4-*NNA*8	2.6194	0.6948	0.0111	-0.0069	0.0108	0.0021	-0.0016	5.1494	0.9163
	Li5-*NNA*6	4.3207	2.3870	0.0120	-0.0083	0.0093	0.0064	-0.0011	1.4511	11.7554
	Li5-*NNA*7	3.5144	1.5819	0.0111	-0.0069	0.0096	0.0050	-0.0013	1.9373	2.5928
	Li5-*NNA*8	3.5167	1.5842	0.0111	-0.0069	0.0096	0.0050	-0.0013	1.9360	2.5994
	*NNA*6-*NNA*7	4.9023	2.5679	0.0120	-0.0083	0.0098	-0.0041	-0.0017	-2.3948	0.7910
			2.3390	0.0111	-0.0069					
	*NNA*6-*NNA*8	4.9019	2.5683	0.0120	-0.0083	0.0098	-0.0041	-0.0017	-2.3960	0.7919
			2.3382	0.0111	-0.0069					
Li_5^-(3)	Li1-*NNA*6	3.9584	2.0731	0.0123	-0.0080	0.0099	0.0042	-0.0014	2.3835	0.2517
	Li1-*NNA*7	2.9561	1.0167	0.0111	-0.0091	0.0103	0.0008	-0.0018	12.3759	0.0132
	Li2-*NNA*6	3.9351	2.0497	0.0123	-0.0080	0.0100	0.0041	-0.0014	2.4013	0.2497
	Li2-*NNA*8	2.9571	1.0175	0.0111	-0.0091	0.0103	0.0008	-0.0018	12.4574	0.0127
	Li3-*NNA*7	2.5716	0.6584	0.0111	-0.0091	0.0108	0.0016	-0.0018	6.7858	0.0018
	Li4-*NNA*6	2.3652	0.4579	0.0123	-0.0080	0.0121	0.0015	-0.0019	8.0873	1.2944
	Li5-*NNA*8	2.5710	0.6576	0.0111	-0.0091	0.0108	0.0016	-0.0018	6.8421	0.0020
Li_5^+(1)	Li1-*NNA*6	2.9926	1.1886	0.0161	-0.0086	0.0147	0.0069	-0.0020	2.1284	0.0002
	Li2-*NNA*6	3.6472	1.8375	0.0161	-0.0086	0.0131	0.0110	-0.0016	1.1904	1.3937
	Li2-*NNA*7	3.6475	1.8379	0.0161	-0.0086	0.0131	0.0110	-0.0016	1.1902	1.3950
	Li3-*NNA*6	3.6482	1.8386	0.0161	-0.0086	0.0131	0.0110	-0.0016	1.1898	1.3968
	Li3-*NNA*7	3.6468	1.8371	0.0161	-0.0086	0.0131	0.0110	-0.0016	1.1907	1.3924
	Li4-*NNA*7	2.9926	1.1886	0.0161	-0.0086	0.0147	0.0069	-0.0020	2.1285	0.0001
	Li5-*NNA*6	3.6463	1.8366	0.0161	-0.0086	0.0131	0.0110	-0.0016	1.1908	1.3915
	Li5-*NNA*7	3.6473	1.8377	0.0161	-0.0086	0.0131	0.0110	-0.0016	1.1902	1.3950
	*NNA*6-*NNA*7	4.3451	2.1726	0.0161	-0.0086	0.0139	-0.0037	-0.0023	-3.8125	0.0002
			2.1725	0.0161	-0.0086					
Li_5^+(2)	Li1-*NNA*6	2.8325	1.0278	0.0160	-0.0119	0.0148	0.0053	-0.0023	2.8110	0.4312
	Li2-*NNA*6	4.1597	2.3032	0.0160	-0.0119	0.0118	0.0058	-0.0016	2.0206	0.2776
	Li2-*NNA*7	4.1583	2.3019	0.0160	-0.0119	0.0118	0.0058	-0.0016	2.0197	0.2777
	Li3-*NNA*7	2.8325	1.0279	0.0160	-0.0119	0.0148	0.0053	-0.0023	2.8085	0.4311
	Li4-*NNA*6	2.8327	1.0280	0.0160	-0.0119	0.0148	0.0053	-0.0023	2.8109	0.4311
	Li5-*NNA*7	2.8327	1.0280	0.0160	-0.0119	0.0148	0.0053	-0.0023	2.8084	0.4311

3. Supplementary Materials S3

Table S3. The Ehrenfest Force (**F**) partitioning scheme measures for the molecular graphs of the Li_m^q (m = 2-5, q = ±1) clusters, where the bonded Li *NCP* separations (Li--Li), the total electronic charge density $\rho(\mathbf{r}_b)$, the Laplacian $\nabla^2\rho(\mathbf{r}_b)$ of the bond critical point (*BCP*), total local energy density $H(\mathbf{r}_b)$, metallicity $\xi(\mathbf{r}_b)$, ellipticity ε, atomic units are used.

Li_m^q	*BCP*	Li--Li	$\rho(\mathbf{r}_b)$	$\nabla^2\rho(\mathbf{r}_b)$	$H(\mathbf{r}_b)$	$\xi(\mathbf{r}_b)$	ε_F
Li_2^-	Li1-Li2	5.0235	0.0127	-0.0121	-0.0033	-1.0427	0.0000
Li_2^+	Li1-Li2	5.8017	0.0126	-0.0129	-0.0033	-0.9705	0.0000
Li_3^-	Li1-Li2	5.6871	0.0101	-0.0078	-0.0020	-1.2914	0.0000
	Li2-Li3	5.6868	0.0101	-0.0078	-0.0020	-1.2913	0.0000
Li_3^+	Li1-Li2	5.5671	0.0126	-0.0088	-0.0025	-1.4240	1.2397
	Li1-Li3	5.5661	0.0126	-0.0088	-0.0025	-1.4233	1.1410
	Li2-Li3	5.5669	0.0126	-0.0088	-0.0025	-1.4238	1.1452
Li_4^-	Li1-Li2	5.5732	0.0109	-0.0055	-0.0019	-1.9708	0.9638
	Li1-Li3	5.5737	0.0107	-0.0048	-0.0019	-2.2532	0.9158
	Li2-Li3	5.5346	0.0101	-0.0030	-0.0017	-3.3456	0.3915
	Li1-Li4	5.5732	0.0109	-0.0055	-0.0019	-1.9708	0.8139
	Li2-Li4	5.5357	0.0102	-0.0044	-0.0018	-2.3123	0.3694
	Li3-Li4	5.5346	0.0101	-0.0030	-0.0017	-3.3459	0.3334
Li_4^+	Li1-Li2	5.8508	0.0115	-0.0078	-0.0022	-1.4617	0.6926
	Li1-Li3	5.8524	0.0115	-0.0078	-0.0022	-1.4629	0.5913
	Li2-Li4	5.8498	0.0115	-0.0078	-0.0022	-1.4615	0.5910
	Li2-Li3	5.1096	0.0124	-0.0067	-0.0026	-1.8334	0.6384
	Li3-Li4	5.8487	0.0115	-0.0079	-0.0022	-1.4607	0.6920
Li_5^-(1)	Li1-Li2	5.2501	0.0105	-0.0048	-0.0020	-2.1594	1.3470
	Li1-Li3	5.2490	0.0104	-0.0048	-0.0020	-2.1586	1.3664
	Li1-Li4	5.2509	0.0104	-0.0048	-0.0020	-2.1575	1.2553
	Li1-Li5	5.2478	0.0105	-0.0048	-0.0020	-2.1584	1.2385
Li_5^-(2)	Li1-Li2	5.5726	0.0119	-0.0085	-0.0024	-1.4038	0.5174
	Li1-Li3	6.0761	0.0101	-0.0058	-0.0016	-1.7454	0.0117
	Li1-Li5	5.4589	0.0098	-0.0042	-0.0018	-2.3314	0.6322
	Li2-Li5	5.4595	0.0098	-0.0042	-0.0018	-2.3322	0.0027
	Li2-Li4	6.0755	0.0101	-0.0058	-0.0016	-1.7449	0.6807
	Li3-Li5	5.5957	0.0100	-0.0064	-0.0019	-1.5554	0.4929
	Li4-Li5	5.5968	0.0100	-0.0064	-0.0019	-1.5563	0.6942
Li_5^-(3)	Li1-Li3	5.5277	0.0111	-0.0091	-0.0024	-1.2120	0.8632
	Li1-Li4	5.6545	0.0106	-0.0074	-0.0020	-1.4301	0.6296
	Li2-Li4	5.6579	0.0106	-0.0075	-0.0020	-1.4278	0.6498
	Li2-Li5	5.5281	0.0111	-0.0091	-0.0024	-1.2123	0.8868
Li_5^+(1)	Li1-Li2	5.9381	0.0135	-0.0076	-0.0022	-1.7721	0.7063

	Li1-Li3	5.9388	0.0135	-0.0076	-0.0022	-1.7727	0.2123
	Li2-Li3	5.0743	0.0109	-0.0016	-0.0020	-6.9281	0.8257
	Li2-Li4	5.9384	0.0135	-0.0076	-0.0022	-1.7723	0.7386
	Li3-Li4	5.9378	0.0135	-0.0076	-0.0022	-1.7718	0.3175
	Li1-Li5	5.9374	0.0135	-0.0076	-0.0022	-1.7715	0.3766
	Li2-Li5	5.0740	0.0109	-0.0016	-0.0020	-6.9312	0.9836
	Li3-Li5	5.0741	0.0109	-0.0016	-0.0020	-6.9304	0.0104
	Li4-Li5	5.9382	0.0135	-0.0076	-0.0022	-1.7722	0.3457
$Li_5^+(2)$	Li1-Li2	5.7836	0.0110	-0.0068	-0.0020	-1.6362	0.0436
	Li2-Li3	5.7826	0.0111	-0.0068	-0.0020	-1.6356	0.0433
	Li1-Li4	5.3186	0.0140	-0.0113	-0.0031	-1.2378	1.2078
	Li2-Li4	5.7826	0.0110	-0.0067	-0.0020	-1.6368	0.0411
	Li2-Li5	5.7817	0.0110	-0.0068	-0.0020	-1.6360	0.0415
	Li3-Li5	5.3182	0.0140	-0.0113	-0.0031	-1.2377	1.2080

4. Supplementary Materials S4.

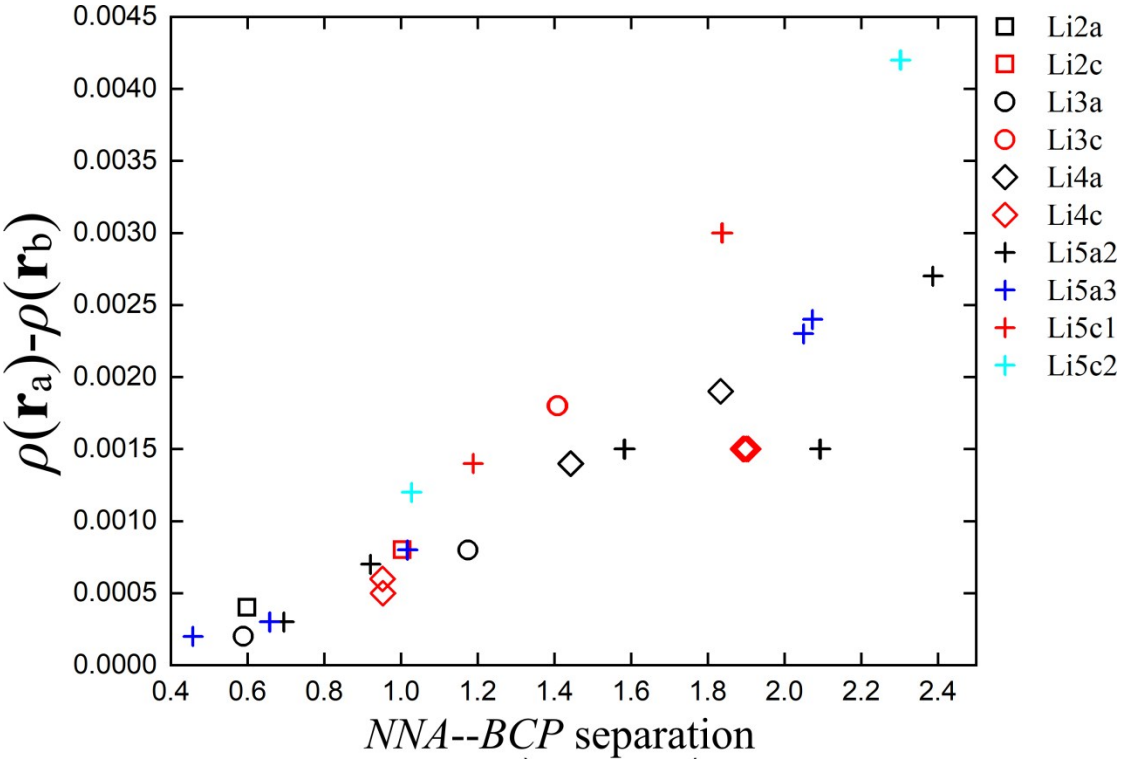

Figure S4. The variation of the total charge density difference ($\rho(\mathbf{r}_a)$-$\rho(\mathbf{r}_b)$) with *NNA-BCP* separation for the Li_m^q (m = 2-5, q = ±1) clusters, see **Table S2** for further information.

5. Supplementary Materials S5.

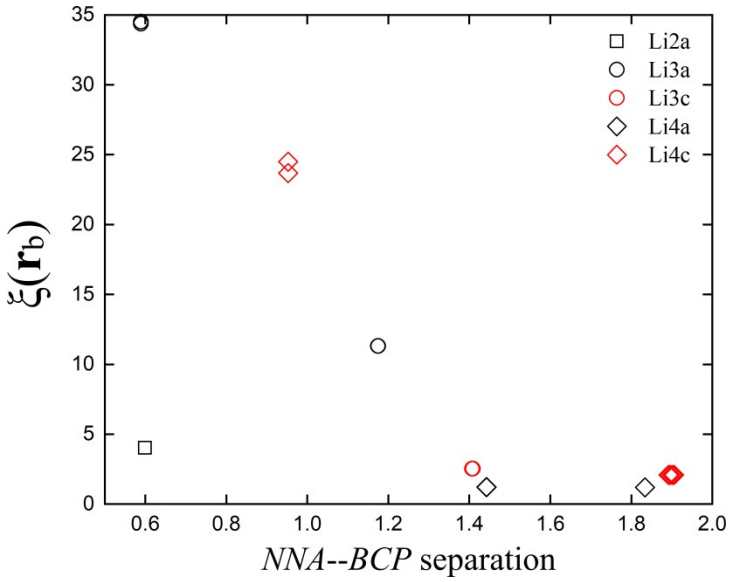

(a)

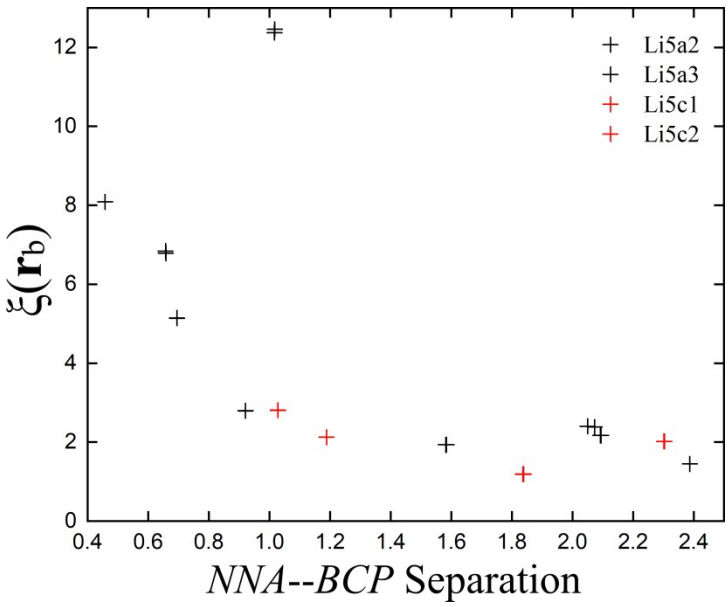

(b)

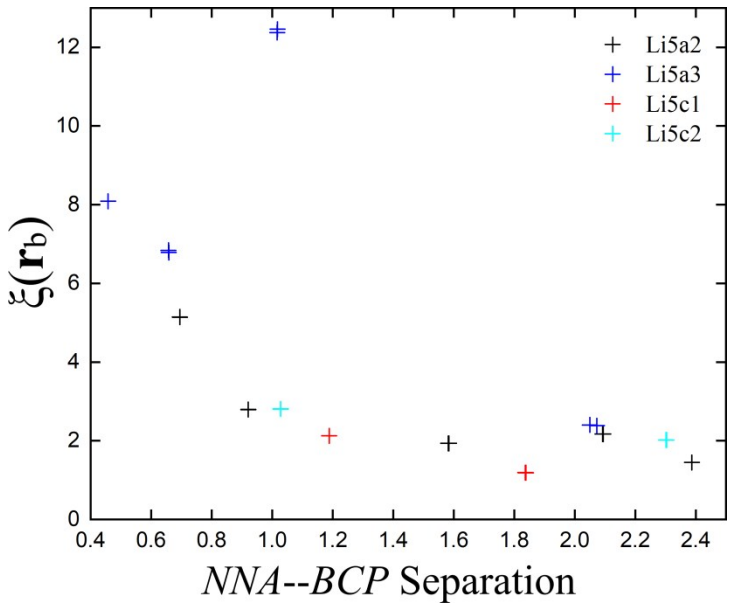

(c)

Figure S5. The variation of the metallicity $\xi(\mathbf{r}_b)$ with the *NNA-BCP* separation for the Li_m^q (m = 2-4, q = ±1) and $Li_5^{\pm}$ clusters are presented in sub-figures **(a)** and **(b)** respectively, see **Table S2** for further information.

6. Supplementary Materials S6.

Table S6. The QTAIM partitioning scheme measures for the molecular graphs of Li_2^- with different *NNA-BCP* separation. See **Table S2** for further information.

Li_2^-	*BCP*	Li--*NNA*/Li	*NNA*--*BCP*	$\rho(\mathbf{r}_a)$	$\nabla^2\rho(\mathbf{r}_a)$	$\rho(\mathbf{r}_b)$	$\nabla^2\rho(\mathbf{r}_b)$	$H(\mathbf{r}_b)$	$\xi(\mathbf{r}_b)$	ε
	Li1-*NNA*3	2.5118	0.5994	0.0112	-0.0084	0.0108	0.0027	-0.0020	4.0185	0.7007
(a)	Li1-*NNA*3	2.4124	0.5549	0.0135	-0.0133	0.0131	0.0010	-0.0027	12.5050	0.0000
(b)	Li1-*NNA*3	2.3124	0.4600	0.0143	-0.0142	0.0140	-0.0005	-0.0031	-26.4523	0.0000
(c)	Li1-*NNA*3	2.2124	0.3492	0.0151	-0.0144	0.0149	-0.0034	-0.0038	-4.3114	0.0000
(d)	Li1-*NNA*3	2.1124	0.1976	0.0158	-0.0133	0.0158	-0.0084	-0.0046	-1.8691	0.0000
(e)	Li1-Li2	4.0248	0.1000	---	---	0.0165	-0.0100	-0.0052	-1.6490	0.0000
(f)	Li1-Li2	3.8248	0.0000	---	---	0.0170	-0.0029	-0.0051	-5.8952	0.0000

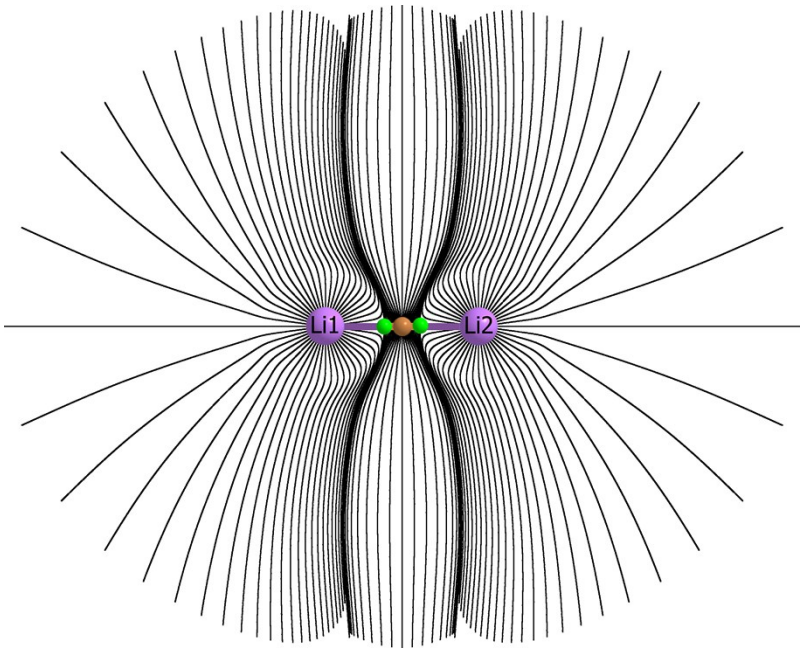

(a)

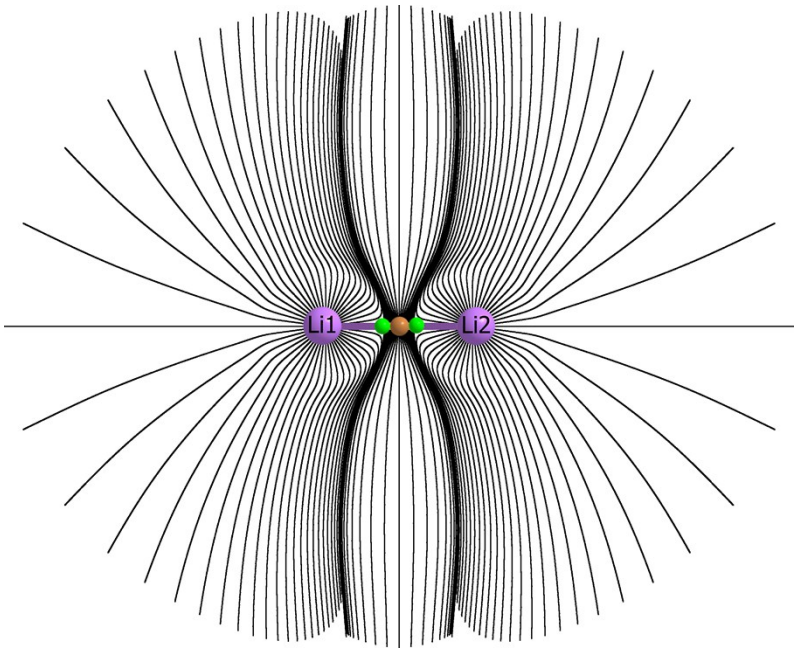

(b)

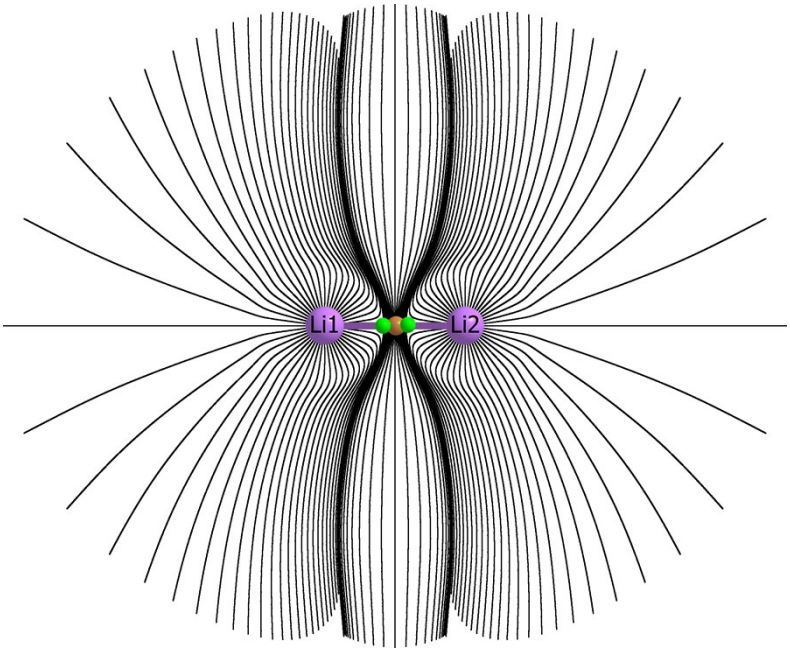

(c)

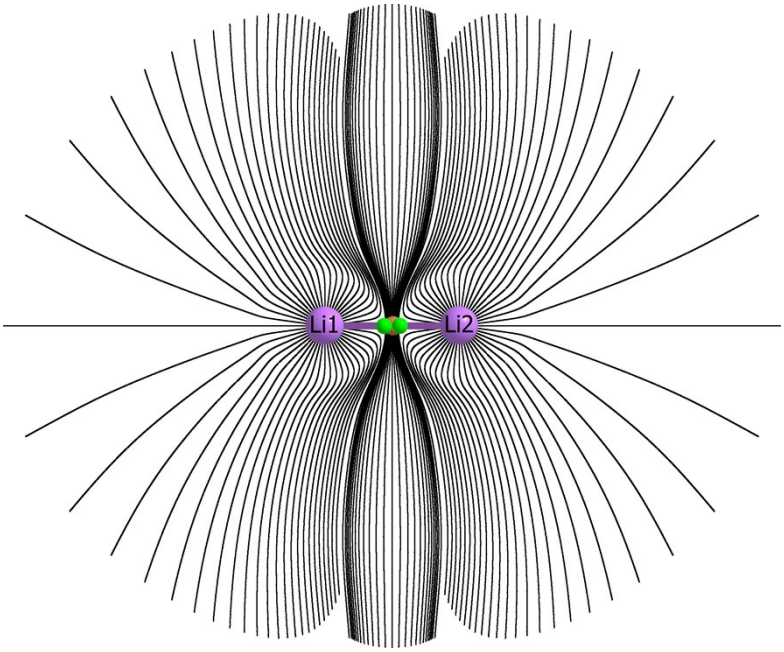

(d)

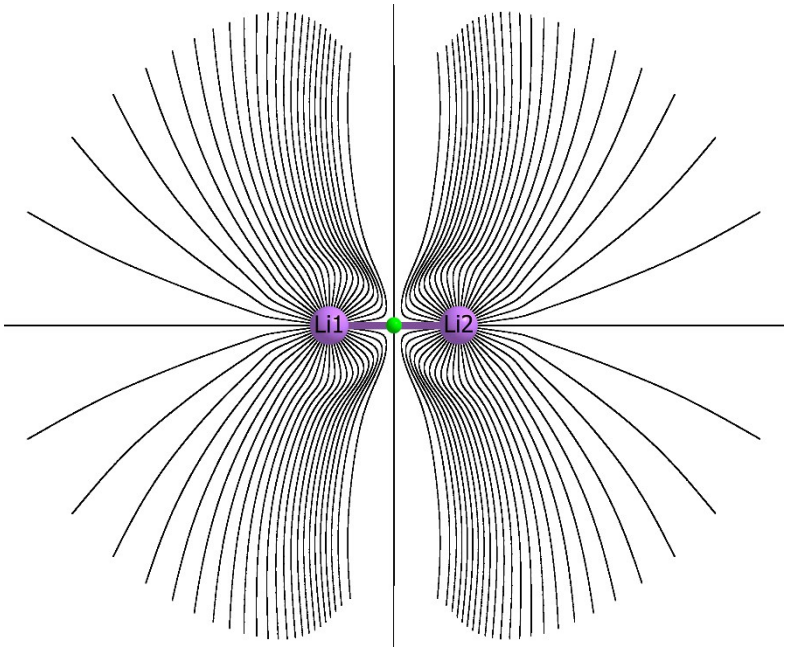

(e)

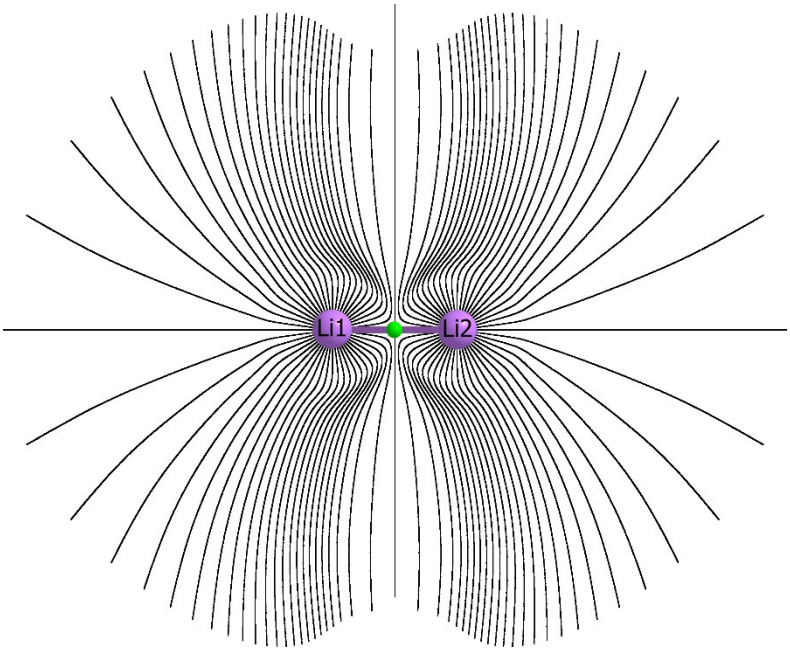

(f)

Figure S6. The QTAIM trajectory maps are superimposed onto the corresponding molecular graphs for Li_2^-. The purple spheres represent the lithium nuclear critical points (*NCP*s), the brown and green represent QTAIM non–nuclear attractors (*NNA*s) and bond critical points (*BCP*s) respectively. See **Table S6** for more information.

7. Supplementary Materials S7.

Table S7. The QTAIM partitioning scheme measures for the molecular graphs of Li_2^+ with different *NNA-BCP* separation. See **Table S2** for further information.

Li_2^+	*BCP*	Li--*NNA*/Li	*NNA*--*BCP*	$\rho(\mathbf{r}_a)$	$\nabla^2\rho(\mathbf{r}_a)$	$\rho(\mathbf{r}_b)$	$\nabla^2\rho(\mathbf{r}_b)$	$H(\mathbf{r}_b)$	$\xi(\mathbf{r}_b)$	ε
	Li1-*NNA*3	2.9009	**1.0041**	0.0126	-0.0129	0.0118	-0.0014	-0.0027	-8.6544	0.0000
(a)	Li1-*NNA*3	2.7433	0.6285	0.0086	-0.0071	0.0085	-0.0047	-0.0020	-1.8251	0.0000
	*NNA*3-*NNA*4	1.3071	0.6535	0.0086	-0.0071	0.0086	-0.0063	-0.0016	-1.3523	0.0000
(b)	Li1-Li2	7.7936	2.0000	---	---	0.0057	-0.0029	-0.0007	-1.9384	0.0000
(c)	Li1-Li2	8.7936	2.5000	---	---	0.0036	-0.0013	-0.0003	-2.8778	0.0000
(d)	Li1-Li2	9.5954	2.9009	---	---	0.0025	-0.0005	-0.0001	-4.1727	0.0000
(e)	Li1-Li2	9.7936	3.0000	---	---	0.0022	-0.0005	-0.0001	-4.6416	0.0000
(f)	Li1-Li2	10.7936	3.5000	---	---	0.0013	-0.0001	0.0000	-9.8456	0.0000

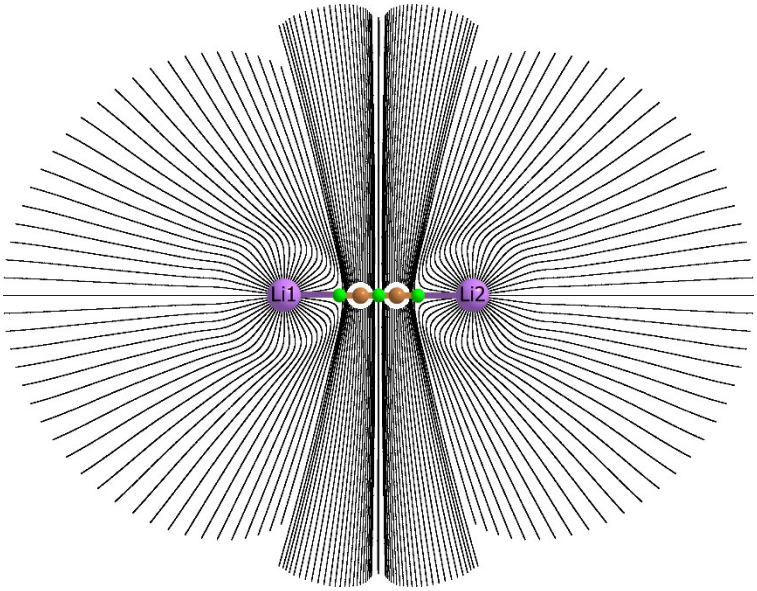

(a)

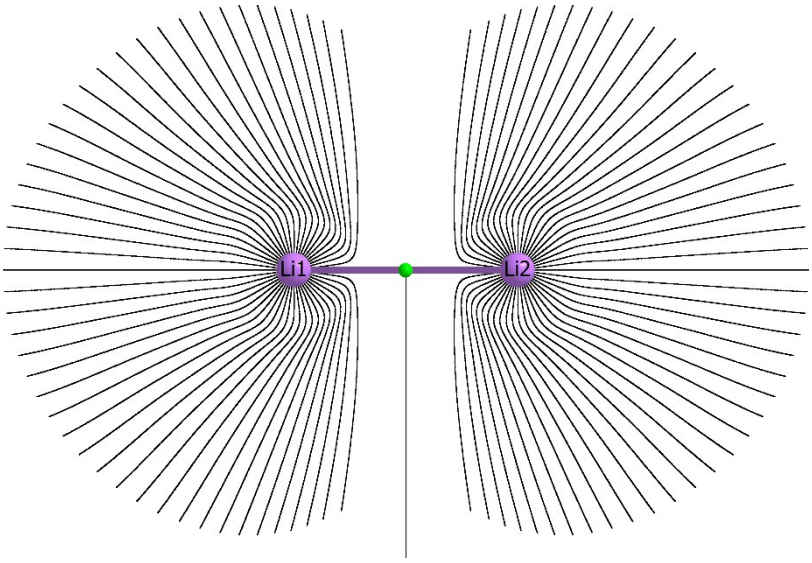

(b)

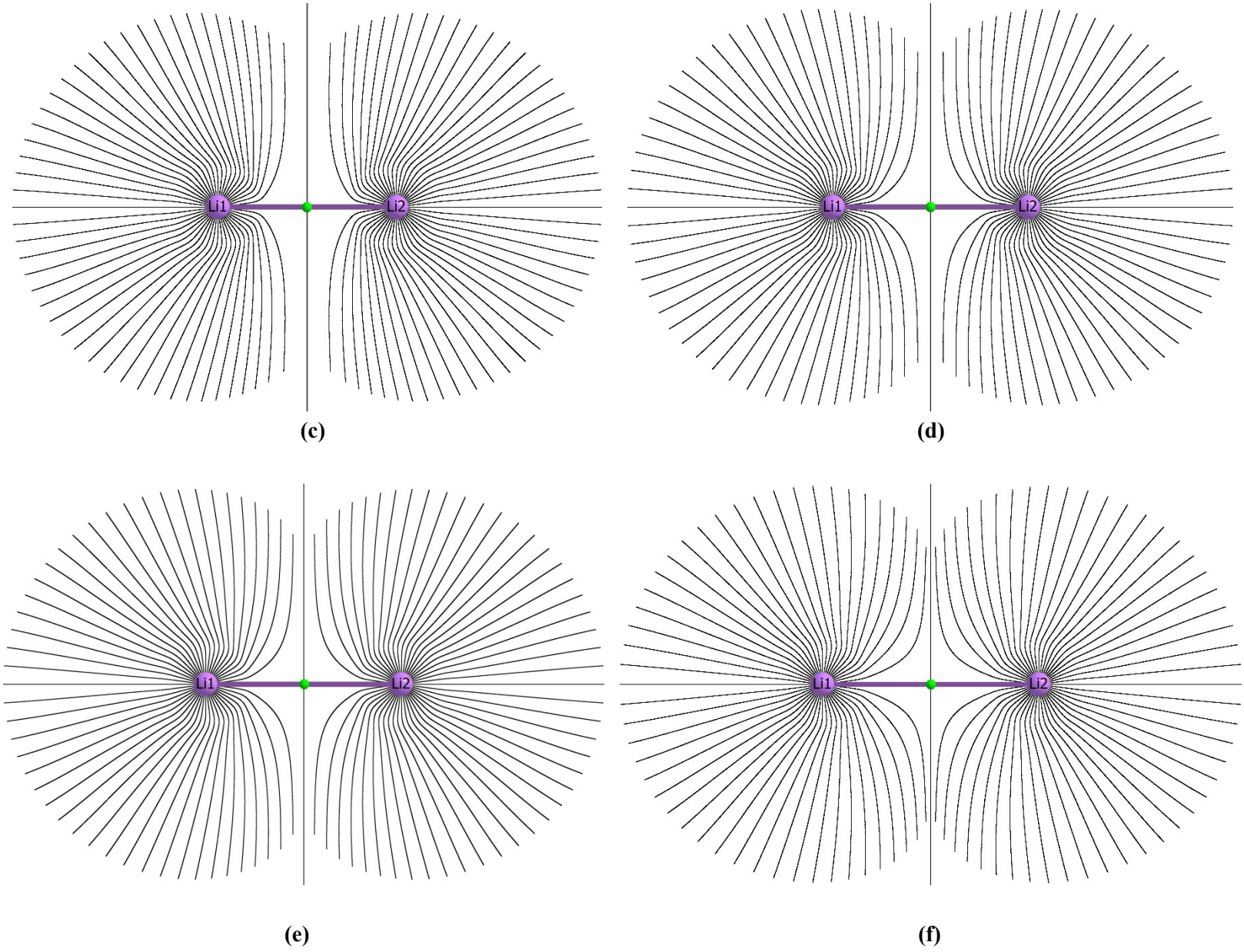

Figure S7. The QTAIM trajectory maps are superimposed onto the corresponding molecular graphs for Li_2^+. The purple spheres represent the lithium nuclear critical points (*NCP*s), the brown and green represent QTAIM non–nuclear attractors (*NNA*s) and bond critical points (*BCP*s) respectively. See **Table S7** for more information.

8. Supplementary Materials S8.

Table S8. The Ehrenfest partitioning scheme measures for the molecular graphs of the Li_2^+ cluster, where the bonded Li *NCP* separations (Li-Li) are presented. See **Table S3** for further information.

Li_2^+	*BCP*	Li--Li	$\rho(\mathbf{r}_b)$	$\nabla^2\rho(\mathbf{r}_b)$	$H(\mathbf{r}_b)$	$\xi(\mathbf{r}_b)$	ε_F
	Li1-Li2	5.8017	0.0126	-0.0129	-0.0033	-0.9705	0.0000
(a)	Li1-Li2	6.0000	0.0117	-0.0113	-0.0028	-1.0346	0.0000
(b)	Li1-Li2	6.5000	0.0096	-0.0079	-0.0020	-1.2225	0.0000
(c)	Li1-Li2	7.0000	0.0079	-0.0054	-0.0014	-1.4536	0.0000
(d)	Li1-Li2	7.5000	0.0064	-0.0037	-0.0009	-1.7391	0.0000
(e)	Li1-Li2	8.0000	0.0052	-0.0025	-0.0006	-2.0955	0.0000
(f)	Li1-Li2	8.5000	0.0042	-0.0016	-0.0004	-2.5492	0.0000
(g)	Li1-Li2	9.0000	0.0033	-0.0011	-0.0003	-3.1457	0.0000
(h)	Li1-Li2	9.5000	0.0026	-0.0007	-0.0002	-3.9747	0.0000
(i)	Li1-Li2	10.0000	0.0020	-0.0004	-0.0001	-5.2367	0.0000
(j)	Li1-Li2	10.5000	0.0015	-0.0002	-0.0001	-7.4656	0.0000
(k)	Li1-Li2	11.0000	0.0012	-0.0001	0.0000	-12.6306	0.0000
(l)	Li1-Li2	11.5000	0.0009	0.0000	0.0000	-38.3576	0.0000
(m)	Li1-Li2	12.0000	0.0006	0.0000	0.0000	39.6864	0.0000
(n)	Li1-Li2	12.5000	0.0005	0.0000	0.0000	13.5058	0.0000

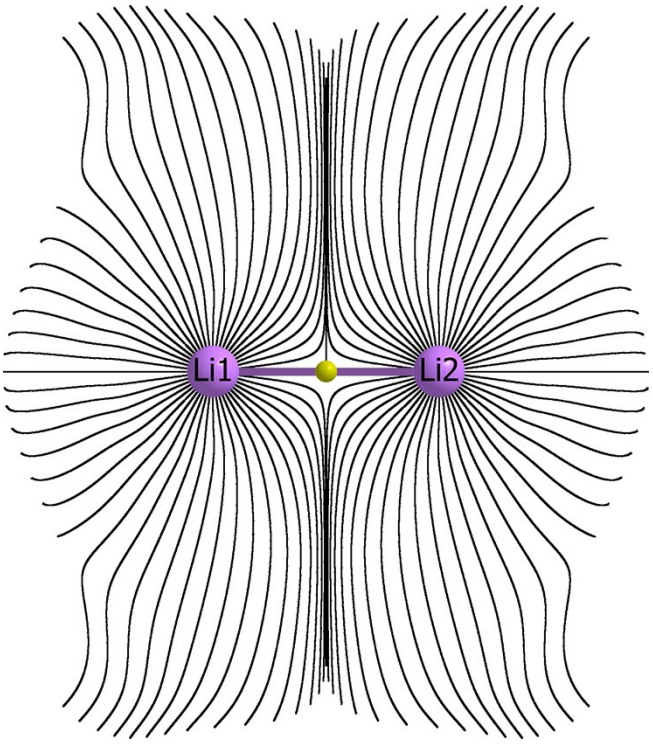

(a)

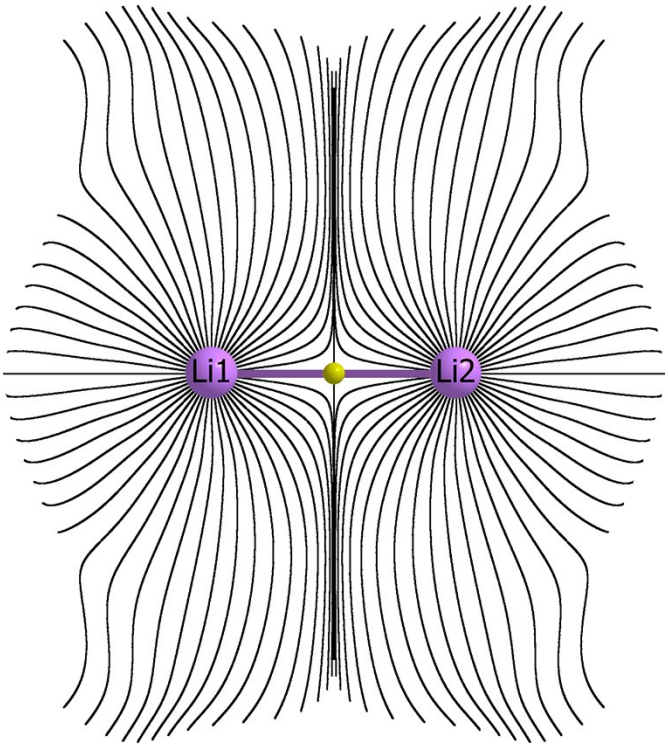

(b)

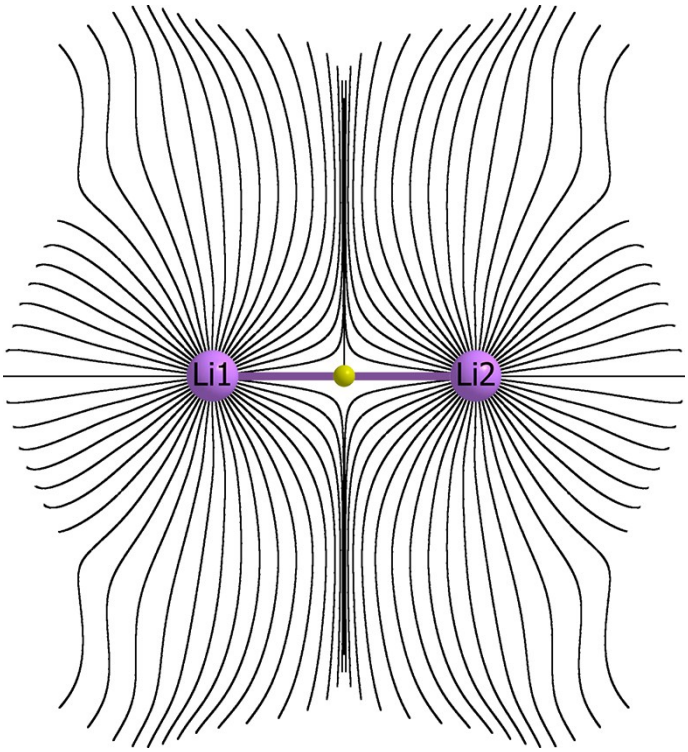

(c)

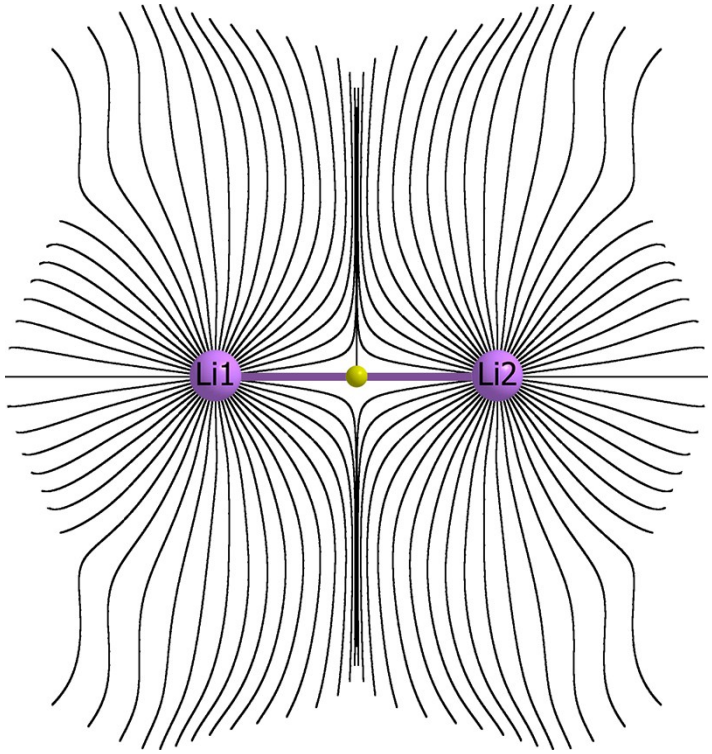

(d)

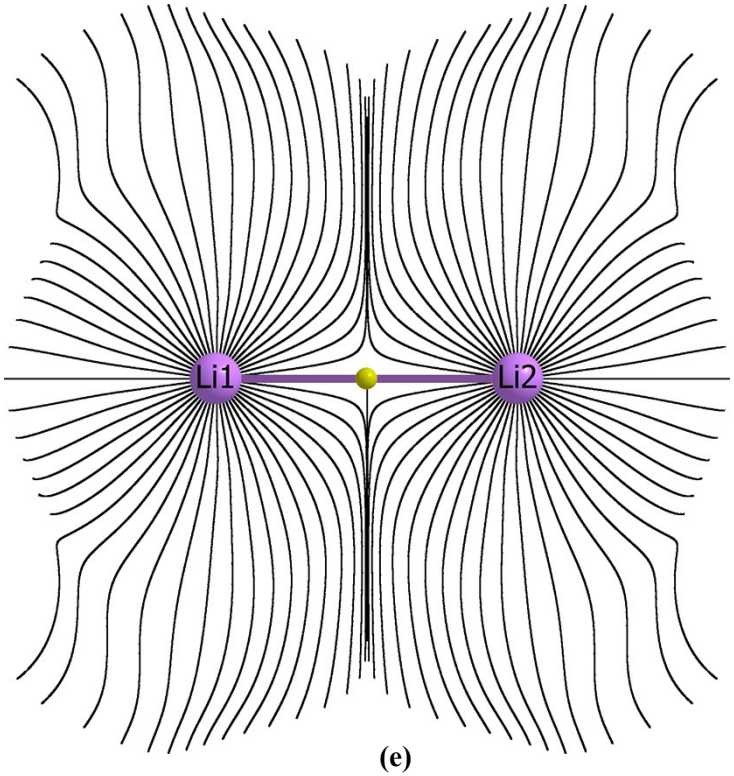

(e)

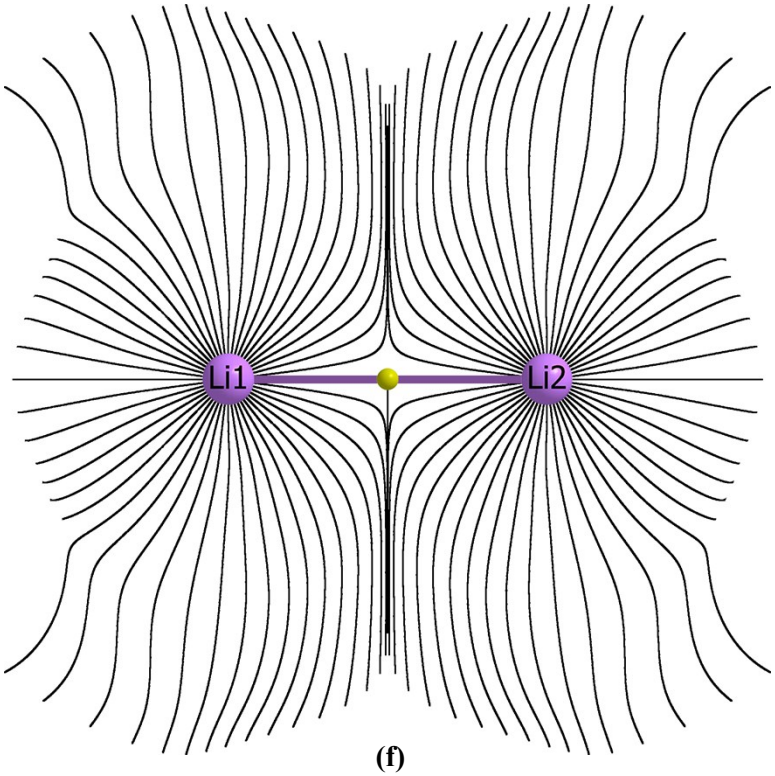

(f)

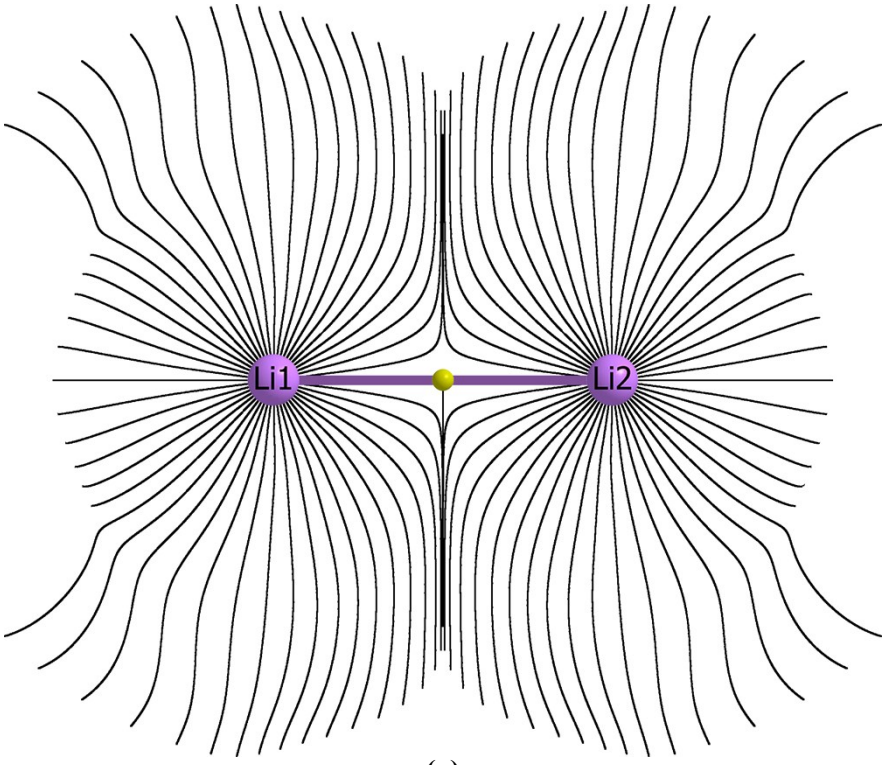

(g)

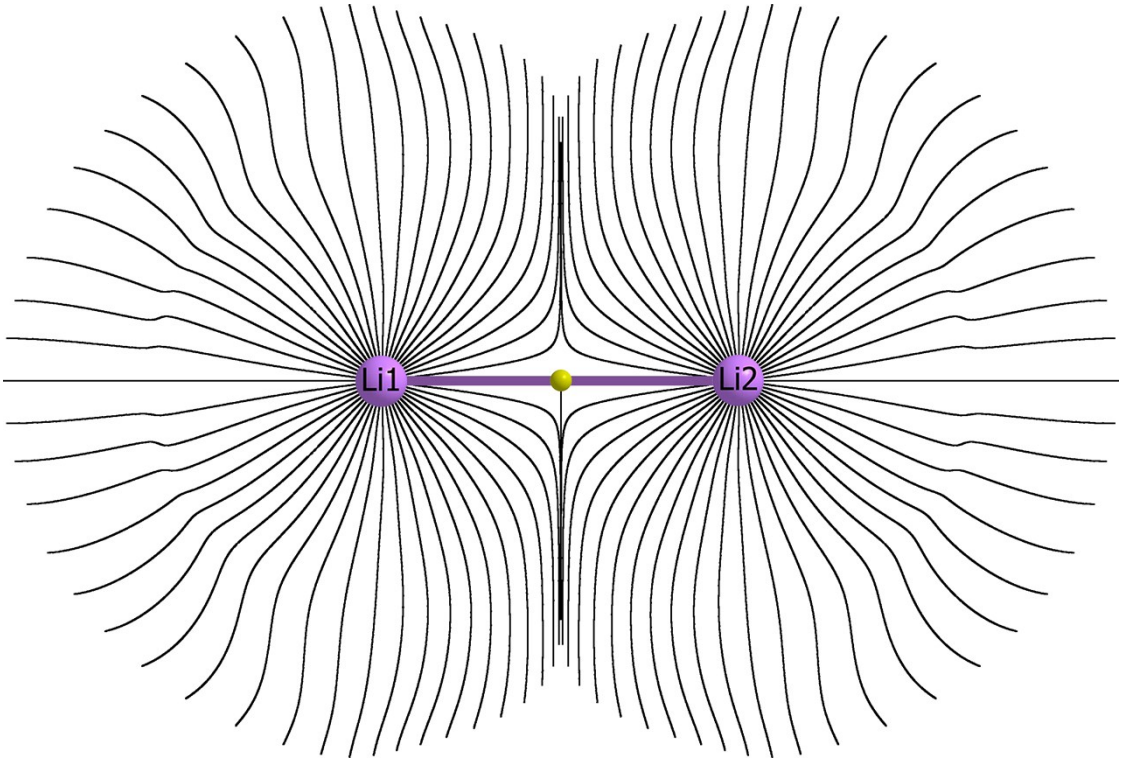

(h)

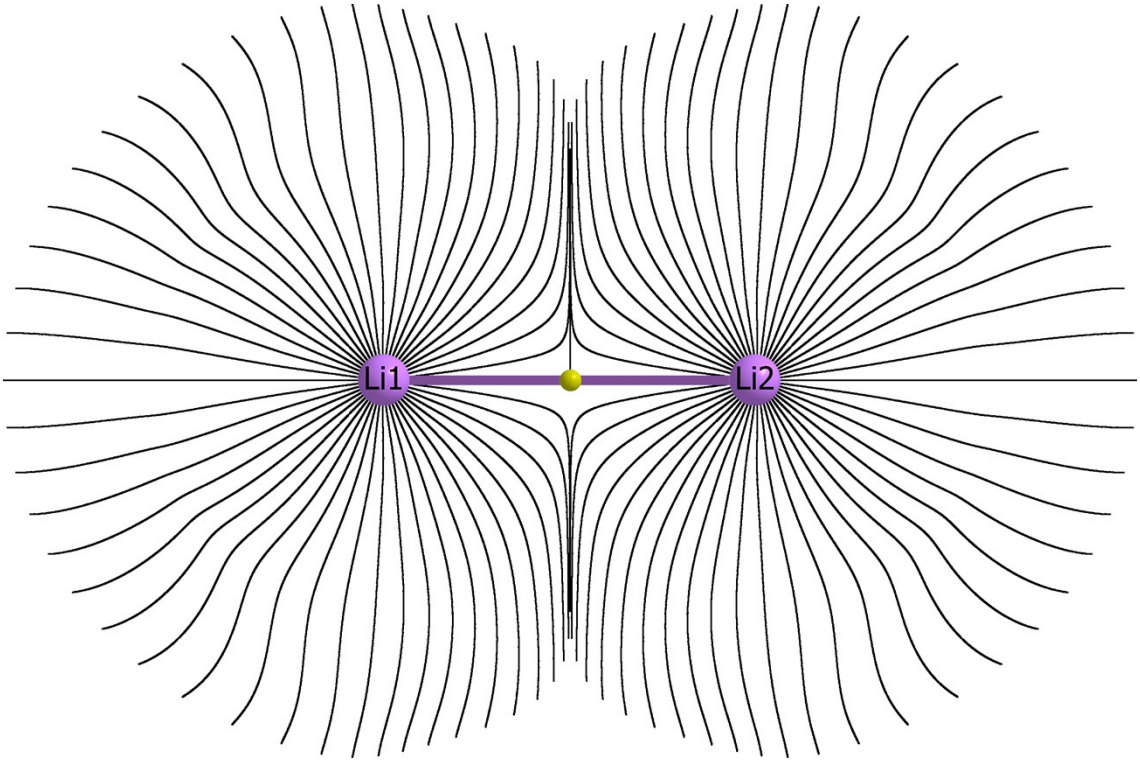

(i)

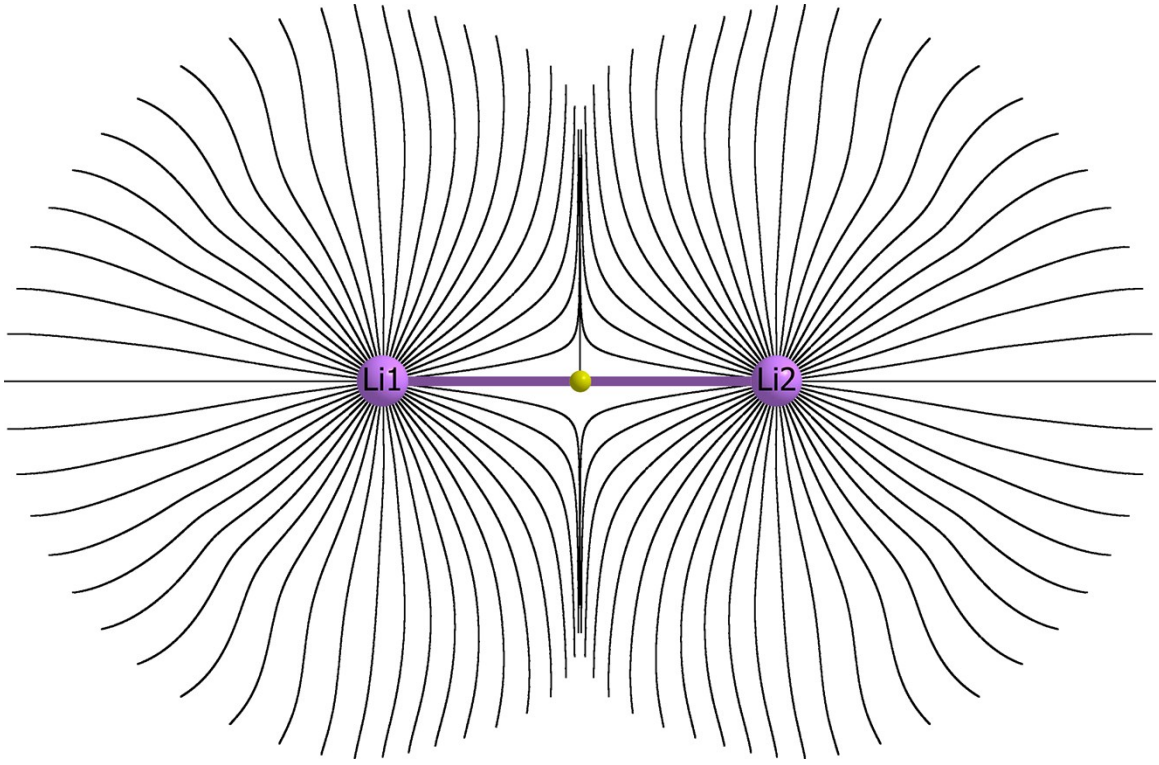

(j)

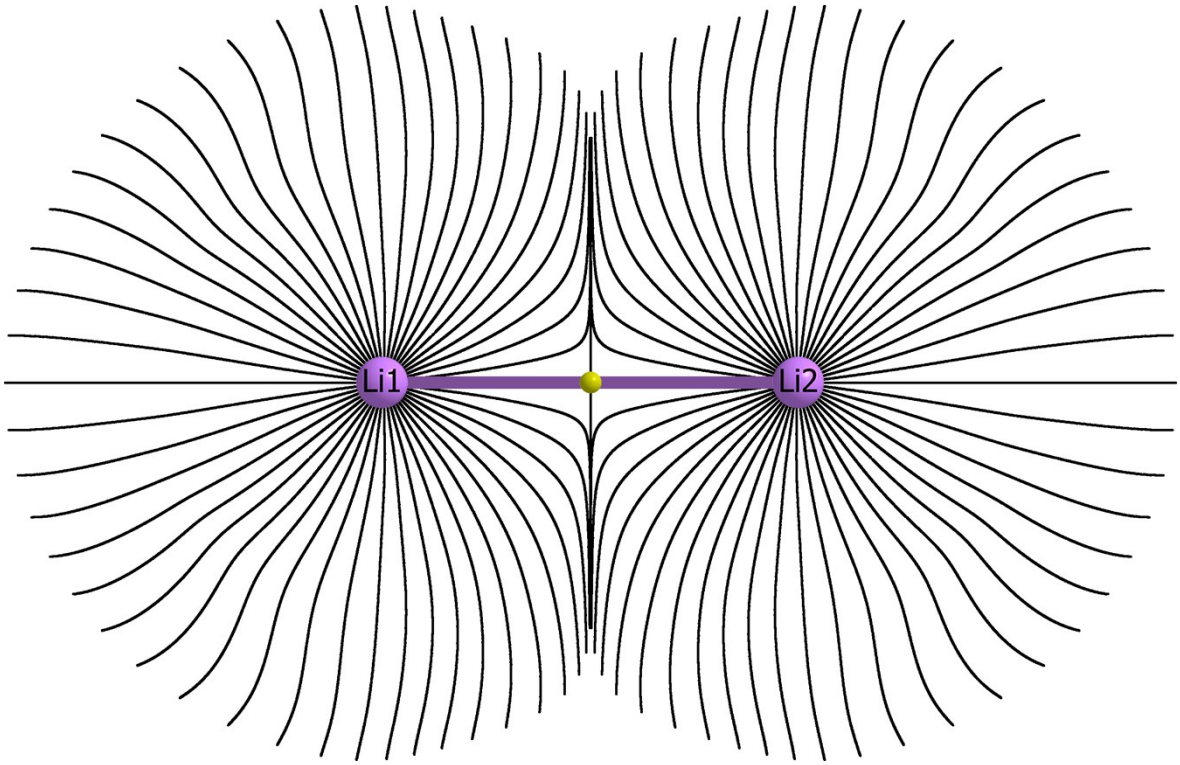

(k)

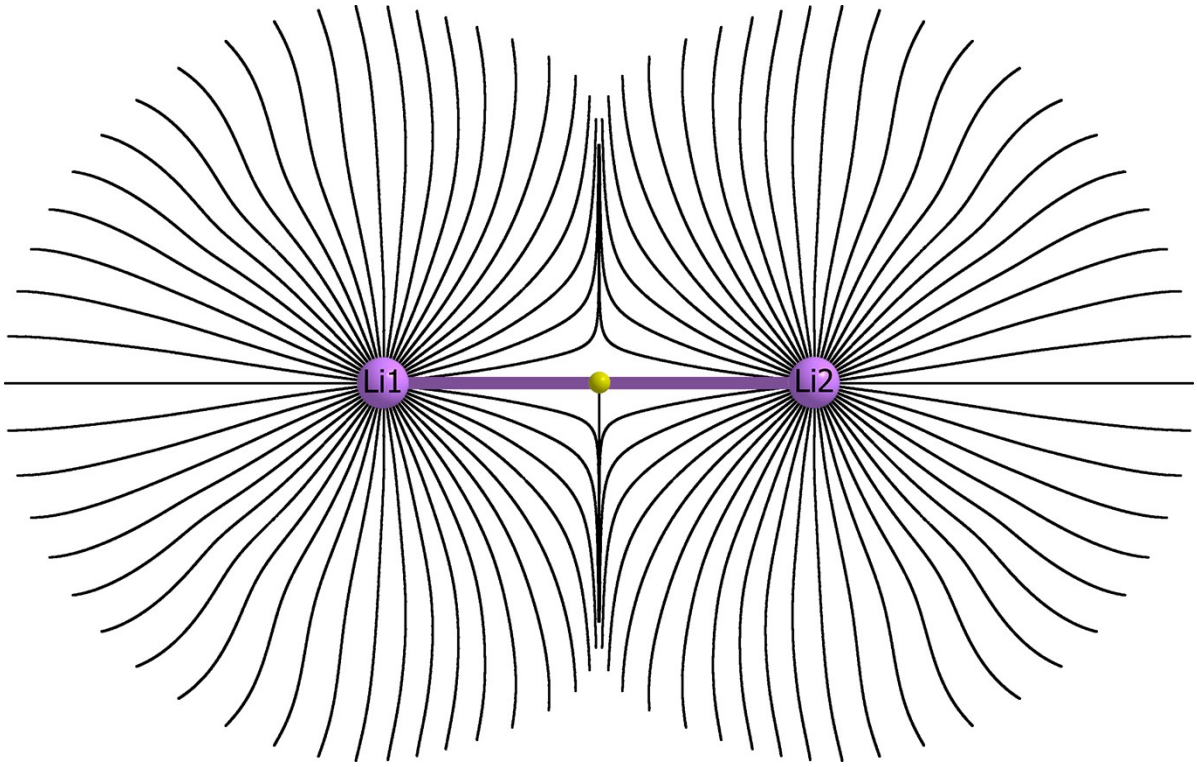

(l)

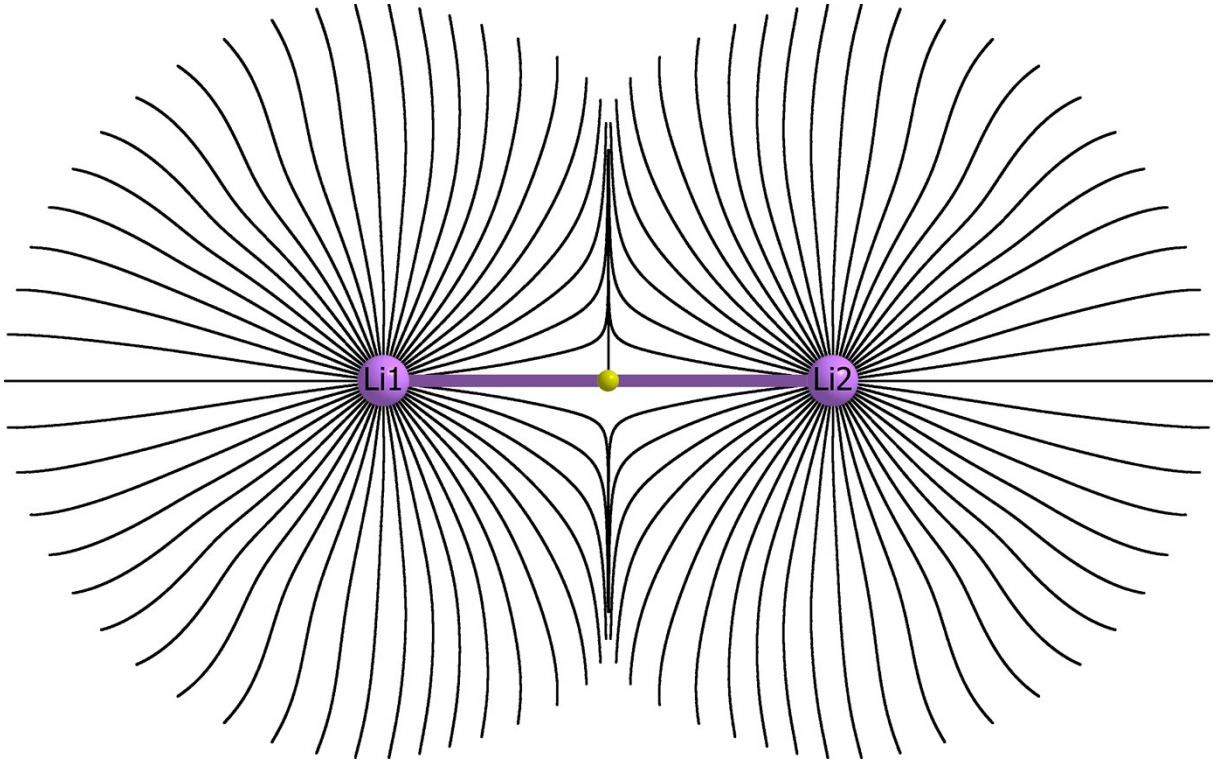

(m)

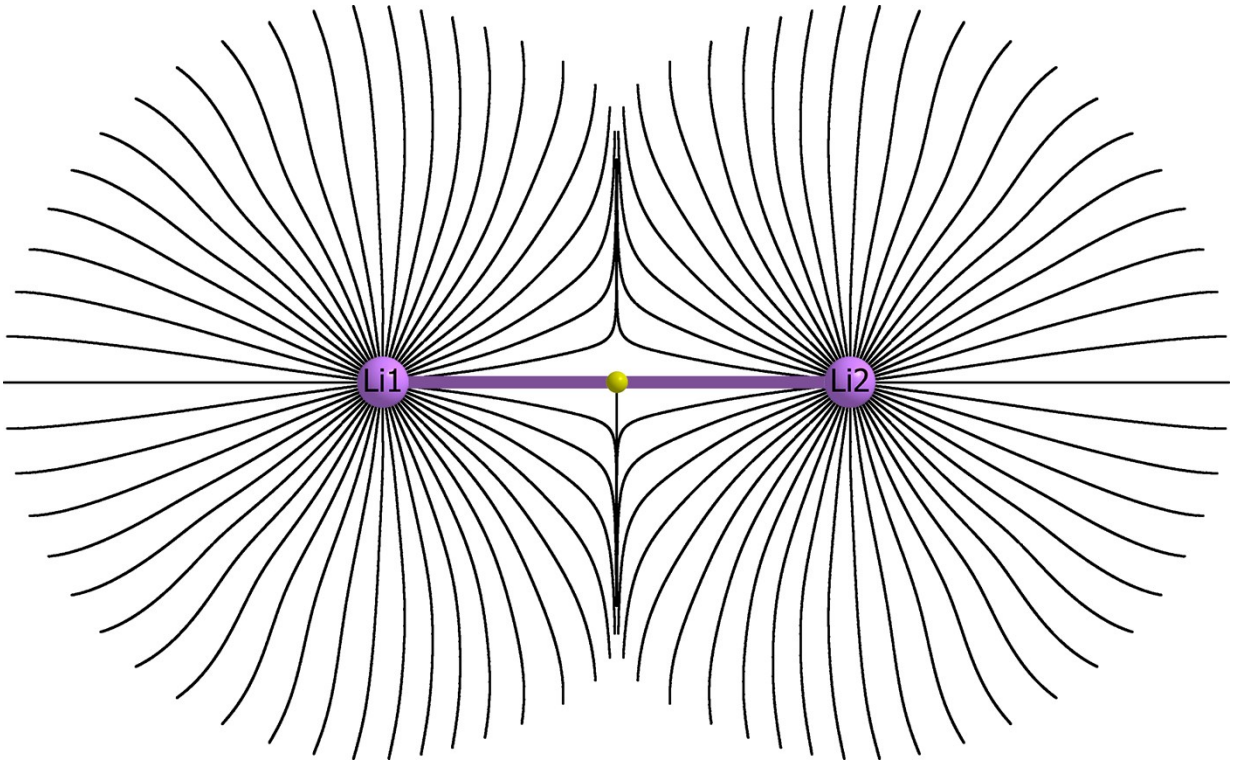

(n)

Figure S8. Ehrenfest Force **F**(**r**) trajectory maps are superimposed onto the corresponding molecular graphs for Li_2^+. The purple and yellow spheres represent the lithium nuclear critical points (*NCP*s) and bond critical points (*BCP*s) respectively. Figures **(a-n)** are corresponding to **Table S8**.